

# ANALYSIS OF UNIFORMITY OF THE DISTRIBUTION OF REINFORCING PHASE IN Cu/SiC COMPOSITE MATERIALS USING $\mu$ CT METHODS

KATARZYNA PIETRZAK<sup>1,2</sup>, ANDRZEJ GŁADKI<sup>†1</sup>, AGATA STROJNY-NĘDZA<sup>1</sup>, TOMASZ WEJRZANOWSKI<sup>3</sup>, KAMIL KASZYCA<sup>✉,1</sup>

<sup>1</sup>Lukasiewicz Research Network - Institute of Microelectronics and Photonics, Poland; <sup>2</sup>Institute of Fundamental Technological Research of the Polish Academy of Sciences, Poland; <sup>3</sup>Warsaw University of Technology, Faculty of Materials Science and Engineering, Poland

e-mail: Katarzyna.Pietrzak@imif.lukasiewicz.gov.pl, Gladki.A@gmail.com,

Agata.Strojny@imif.lukasiewicz.gov.pl, Tomasz.Wejrzanowski@pw.edu.pl,

Kamil.Kaszyca@imif.lukasiewicz.gov.pl

(Received February 14, 2018; revised November 24, 2020; accepted April 2, 2021)

## ABSTRACT

Tomography allows embedding of one space in another, especially  $\mathcal{R}^2 \rightarrow \mathcal{R}^3$ , and observation of the nature of the volumetric internal composite structure. Now, not only a simple interpretation is expected of geometry defined via single thresholds of structures. The binary segmentation used for numerical structure analysis requires more detailed presentation. This paper shows an example of image analysis techniques applied to study the homogeneity of two-phase material. Using tomography analysis, the results of the homogeneity of the SiC particles with 10vol.%, 20vol.%, 30vol.%, 40vol.% volumetric bulk density of Cu/SiC composites are presented. Finally, for two independent coordinate systems, the distribution of SiC particle masses and their total moments of inertia were determined. The results confirmed that for well-mixed composite powders the homogeneity of the reinforcing phase is expected in samples with a SiC volume near 30vol.%. In this case, segregation by translation and rotation of SiC particles in the matrix, during the sintering process is restricted.

Keywords: Cu/SiC composite materials, image analysis, isotropy, uniformity.

## INTRODUCTION

Copper, with its good thermal and electrical conductivity, corrosion resistance and high melting point, is commonly used in the following industries: energy, electronics, automotive and aviation. However, its relatively low mechanical strength, both at low and high temperatures, limits the possibility of using pure copper (Campbell F.C., 2010). This is why various forms of reinforcing phases are used for the copper matrix, i.e. particles, flakes, fibers or whiskers (Jarzabek D. *et al.*, 2016; Pietrzak K. *et al.*, 2016; Iguchi M. *et al.*, 1982; Yoshida K. *et al.*, 2004 Weber L. *et al.*, 2007). One of such phases is silicon carbide (SiC) which makes the composite material Cu/SiC similar to pure copper, but more mechanically durable. The addition of SiC as the reinforcement reduces also its coefficient of linear expansion (Singh H. *et al.*, 2015; Chmielewski M. *et al.*, 2017; Zhan Y. *et al.*, 2003). In most cases isotropic mechanical strength and linear expansion both are expected (Besharati M.K. *et al.*, 2011; Barmouz M. *et al.*, 2014; Srinivasan C. *et al.*,

2015). Gradient or laminated materials are an exception. Fabrication of isotropic structures with the use of powder metallurgy in composites with a molecular reinforcing phase requires proper selection of shapes and sizes of powder particles as early as in the mixing process (Gan K. *et al.*, 2008; Zaman M. *et al.*, 2012). Sintering a mixture of Cu and SiC powders sometimes requires certain modifications. Due to the interaction between Cu and SiC, the surface of SiC grains can be modified by coating with e.g. molybdenum (Schubert Th., *et al.*, 2007) or tungsten (Chmielewski M. *et al.*, 2017). Quantitative structural analysis of composite materials, including the measurements of phase compositions, the size of grains and molecules, their surface, volume, shape, uniformity and isotropy (Gawdzińska K. *et al.*, 2010) are conducted via two methods. The first method uses all the methodological gains of the so-called Quantitative Metallography (QM). QM methods make it possible to estimate various geometric parameters of structures, based on the analysis of 2D images (Underwood E.E. 1970; DeHoff R.T. *et al.*, 1961; Głowacz E. *et al.*,

2008; Xu Y.H. *et al.*, 2003; Wejrzanowski T. *et al.*, 2010; Wejrzanowski T. *et al.*, 2008). The second group of methods uses computer tomography (CT) at various resolutions in order to visualize structure and perform quantitative analysis in 3D space. Thanks to rapid development of computers X-ray tomography ( $\mu$ CT) and 3D image analysis is a valuable tool for the analysis of materials at various length scales. Applications, advantages and limitations of CT methods have been extensively reviewed in the article „Quantitative X-ray tomography” (Maire E. *et al.*, 2014). The paper shows an example of the use of algorithms for particles, represented by the images of their binary masks. After imaging in 3D space, the

centers of mass of the particular SiC particles, as well as their volumes, were determined. These parameters were used for the analysis of isotropy and uniformity of distribution of SiC reinforcing phase in Cu-SiC composites with the volume fraction of SiC from 10-40%. Cu/SiC composites were manufactured using the powder metallurgy method. The copper powder (NewMet Koch) was used, as well as the Sika Saint-Gobain silicon carbide. Fig. 1 presents the SEM image of the Cu-SiC powder mixture, the shape factors of projections of powder particles on a measuring surface, as well as the distributions of values of Feret's diameters.

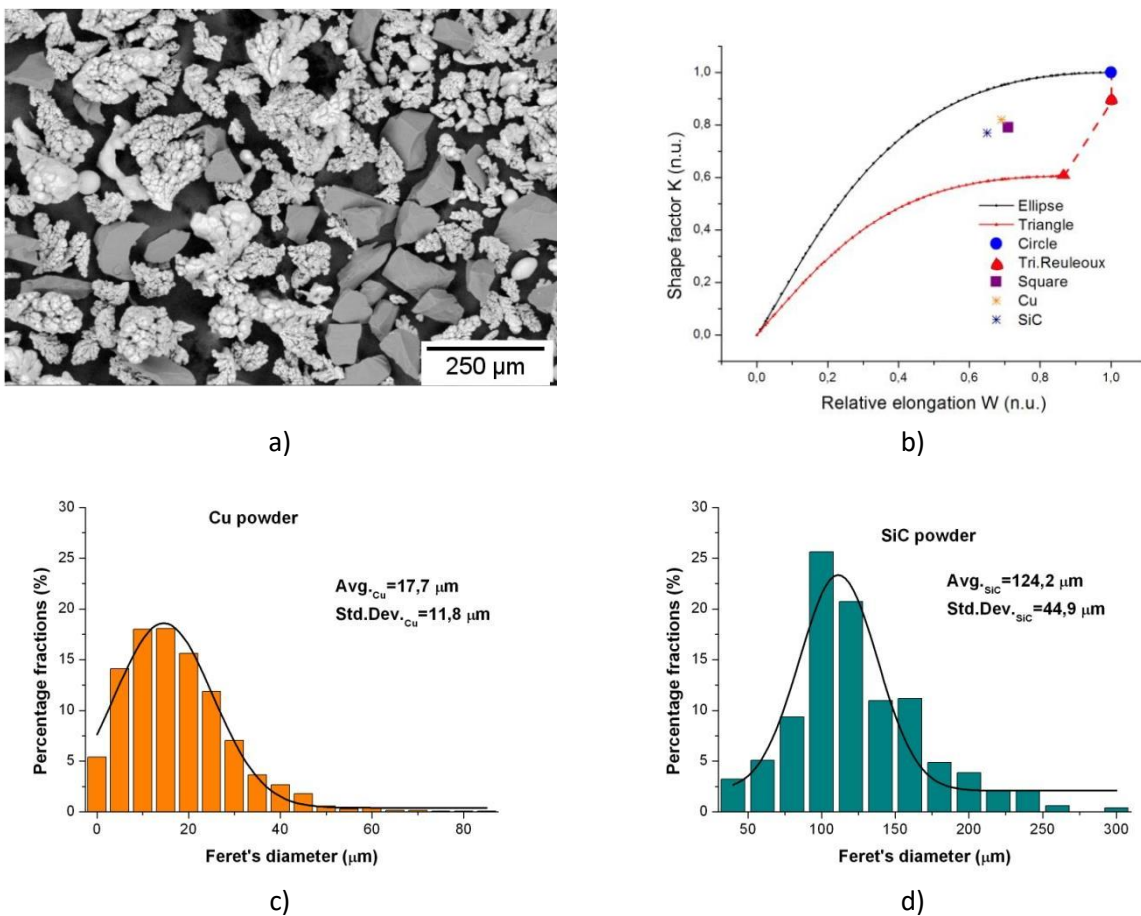


Fig. 1. a) SEM image of Cu (light) and SiC (gray) particles; b) Shape parameters in 2D space of convex shapes for particles projections; c) Feret's diameters distribution of Cu powder particles; d) Feret's diameters distribution of SiC powder particles.

The granulometric analysis of powders based on optical microscopy images with the resolution of 2.1  $\mu$ m/pixel was conducted using Vision PE by CLEMEX. For the shape analysis, modified KS 300 Zeiss procedure libraries were used. In the direct measurements - Clemex – the average Feret's diameter

was determined, from the projections of the image of a single 2D particle in coordinate systems rotated in a range of angles 0-157.5° with the step of 22.5°. The shape factor of particles was determined from their binary masks consisting of convex polygons - KS 300 procedure. Convex areas of polygons  $A_C$  were

measured, as well as the corresponding convex perimeters  $P_C$  and both Feret's diameters  $d_{\min}$  and  $d_{\max}$ . The following equation were used to calculate shape factors:  $= 4\pi \frac{A_c}{P_c^2}$ ;  $K \in (0; 1]$ ;

$$\text{as well as } W = \frac{d_{\min}^F}{d_{\max}^F}; W \in (0; 1],$$

where values create the space of flat convex shapes, limited with strings of ellipses, triangles and figures with constant width – circles and Reuleaux triangles – Fig. 1b. Powders used in this study consisted with particles with the average Feret's diameter:  $\overline{d}_{Cu}^F = 17.7 \mu\text{m}$  and  $\overline{d}_{SiC}^F = 124.2 \mu\text{m}$ . The shape factors of both types of powder particles were approximately square  $\left[ \begin{matrix} K = 0.71 \\ W = 0.79 \end{matrix} \right]$  and were respectively:

$$\left[ \begin{matrix} K_{SiC} = 0.77 \\ W_{SiC} = 0.65 \end{matrix} \right] \text{ and } \left[ \begin{matrix} K_{Cu} = 0.82 \\ W_{Cu} = 0.69 \end{matrix} \right].$$

Particles of Cu and SiC powders had similar shapes. The difference between both powders particle size was in the range of one order of magnitude. The range of Feret's diameters of copper powder was a subset of the range of SiC diameter ranges. Due to the similarity in shapes and sizes of particles of both powders, the probability of their uniform mixing was very high. Powders were mixed in a Fritsch planetary mill, and the composite material was sintered using the SPS method. Following composites were manufactured:

$$Cu - x\%_{vol.}SiC, x = \{10, 20, 30, 40\}$$

The central areas (2x2x2 mm) of the samples were analyzed with an XRADIA XCT-400 X-ray microtomography ( $\mu\text{CT}$ ). The source of radiation was an X-ray lamp, operating at 150 kV with the current of 64  $\mu\text{A}$ . From every sample 1000 projections were obtained in the angular position  $0 \div 180^\circ$ . The linear scanning resolution was 2  $\mu\text{m}$ .

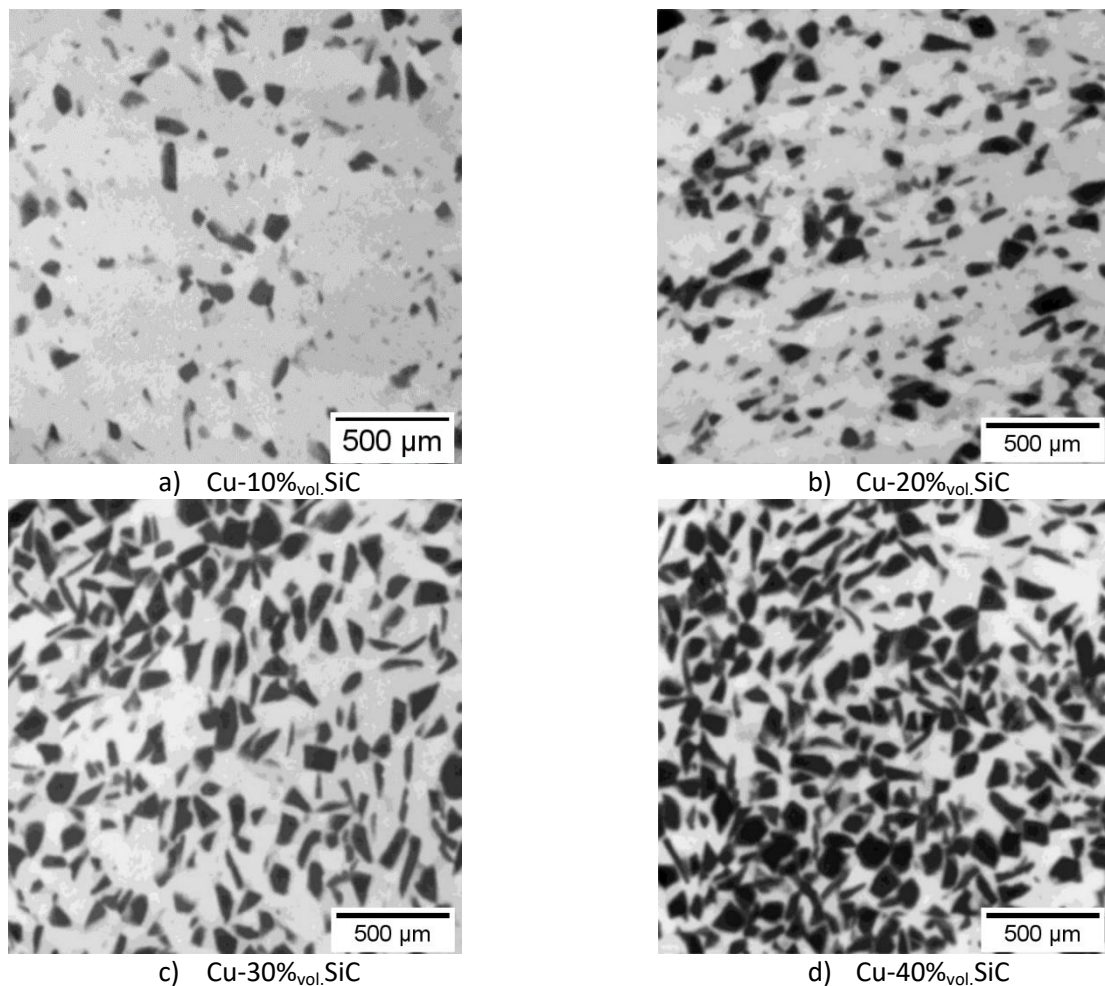


Fig. 2.  $\mu\text{CT}$  single images of the SiC/Cu composite with various SiC volume fraction.

In Fig. 2 examples of the single images from the set of tomographic data are presented for materials with varying volume fraction of reinforcing phase. One of the basic parameter which might be calculated is the volume fraction of SiC phase, which is determined by summing up the number of pixels/voxels inside objects identified as SiC. More complicated analysis is related with isotropy and uniformity of distribution of SiC phase within the Cu matrix. The analysis of isotropy and uniformity follows a certain convention (Figs. 3, 4). Uniformity results from isotropy, not the other way around. Isotropy depends on the choice of a coordinate system (Fig. 4b). In order to study isotropy and uniformity of SiC particles in a Cu matrix, the individual position of each particles and their volume (mass) have to be calculated.

If the space is isotropic around observer X, the densities at 1, 2, and 3 are equal. Drawing spheres of different radii around observer Y, it is seen that the region within the spherical shell around Y has to be homogeneous. Credit: J.A. Peacock 1999, Cosmological Physics, Cambridge University Press

The separation of particles in each of the 4000 photos was conducted via analyzing binary masks overlaid on particle images. Separation was conducted using the procedures of the Clemex Vision PE program.

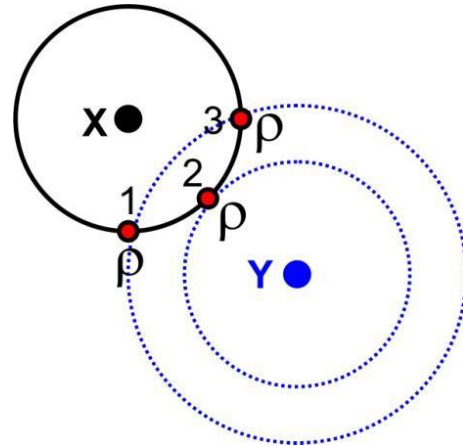


Fig. 3. Homogeneity follows from the isotropy around two points.

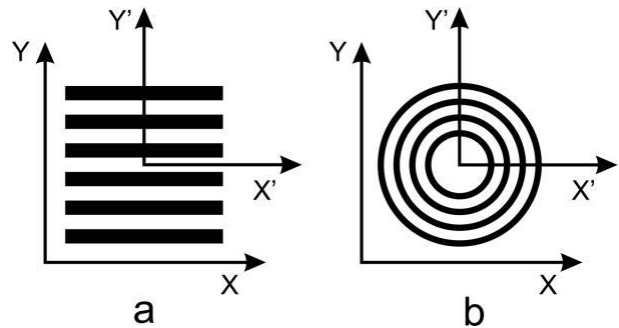
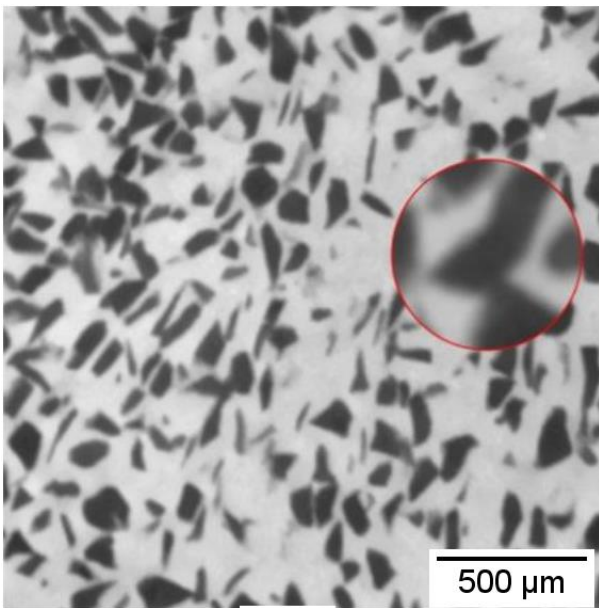
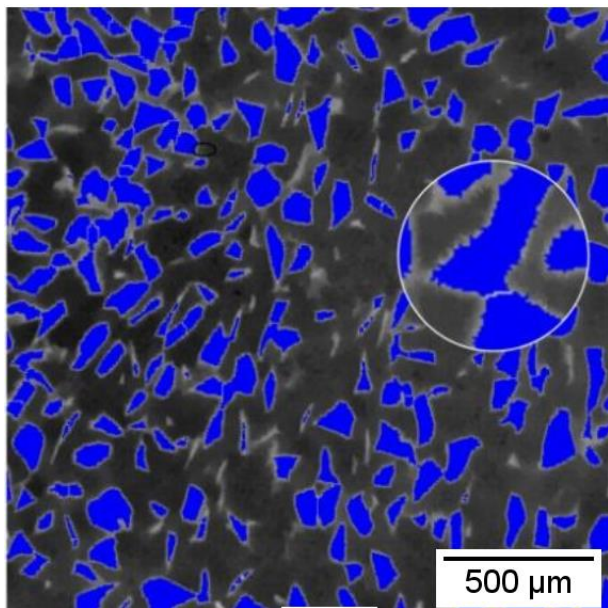


Fig. 4. The space in a) is homogeneous but not isotropic in both coordinate systems. In b) the space is isotropic for X'Y' coordinate; not isotropic for XY coordinate system.



a)



b)

Fig. 5. a) Real tomography image of SiC particles; b) binary mask of negative image. Inside the circles are enlarged fragments of grains with a white separation line



Fig. 5 presents a tomography image, as well as its negative with an overlaid binary mask. The circles include zoomed-in areas with a visible separation of two objects. Sequences of binary maps were analyzed with 3D Slicer (<https://www.slicer.org>) and Fiji (<https://fiji.sc>), with our own procedures written in C++. The  $V_i$  volume of particles was determined, as well as the coordinates of their centers of mass  $\langle x_i | y_i | z_i \rangle$ ; relative to the center of the sample and the external coordinate system. The coordinates of a center of mass were analyzed, in a coordinate system bound to the center of the sample, as well as the moments of inertia relative to an external coordinate system. The volume fraction of SiC phase was determined from the equation:

$$V_{SiC}(\%) = \frac{\sum_i V_i(SiC)}{V(Specimen)} \times 100\%$$

The coordinates of the centers of mass:

$$m_{0x(y,z)} = \frac{\sum_i m_i \langle x_i | y_i | z_i \rangle}{\sum_i m_i} = \frac{\sum_i \rho V_i \langle x_i | y_i | z_i \rangle}{\sum_i \rho V_i} \\ = \frac{\sum_i V_i \langle x_i | y_i | z_i \rangle}{\sum_i V_i}$$

Moments of inertia were determined from the equation:

$$I_x = \sum_i (\rho V_i \times x_i^2); \\ I_y = \sum_i (\rho V_i \times y_i^2); \\ I_z = \sum_i (\rho V_i \times z_i^2);$$

For the representation of data, the quotient of moments was used:

$$M_{x/y} = \frac{I_x}{I_y} = \frac{\sum_i (\rho V_i \times x_i^2)}{\sum_i (\rho V_i \times y_i^2)}$$

For analysis purpose, simplification and increase of sensitivity we assumed dark-phase (SiC) density unity and only dark-phase center of geometrical mass and geometrical moments of inertia were calculated (Cu phase was intentionally omitted).

## RESULTS

Measuring sets  $S(V_i; x_i; y_i; z_i)$ , depending on the percentage share of the SiC reinforcing phase, had the following range of SiC particle count: from  $7.0 \times 10^3$  for Cu/10vol.%SiC to  $3.8 \times 10^4$  for a Cu/40vol.%SiC

sample. 3D visualization of such large groups of variables, in particular the space occupied by SiC particles, is completely unintelligible. This is why they are graphically represented as values indicating layers with the volume of  $= (X \times Y) \times \Delta Z = (2000 \mu m \times 2000 \mu m) \times 42.5 \mu m$ , where  $(X, Y)$  are the full dimensions of a sample,  $\Delta Z$  is the thickness of a layer in the direction of the Z axis. The volume fraction changes of SiC phase along Z direction is presented in Fig. 6, and the numerical results are shown in Table 1.

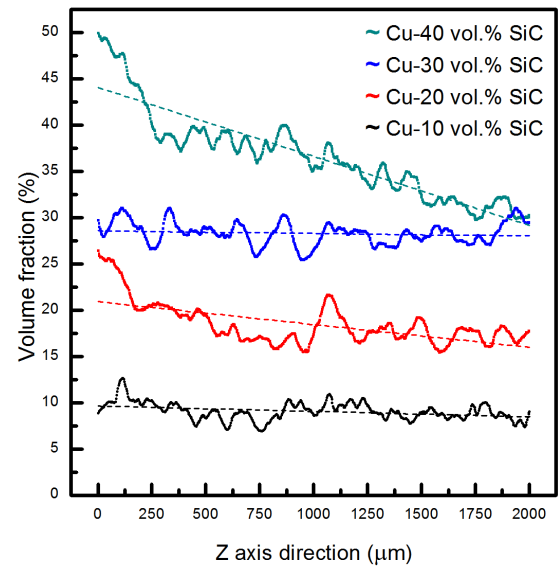


Fig. 6. SiC density results calculated for 42.5  $\mu m$  thick layers

The average volume fraction of the SiC reinforcing phase in all of the studied samples is lower than that resulting from their preparation procedure. There are two significant sources of error resulting from the tomographic measurement. The first concerns overlaying binary masks over actual images, the second – tomography resolution. In Fig. 5b, in the negative image with overlaid binary masks, light spots can be clearly seen, as well as halos around particles that are not included in the dark blue masks. These areas are on the detection sensitivity threshold of the shades of grey related to the inside of SiC particles. The detection scale ranges from 0 for black to 255 for white. On the sensitivity threshold a change of the detection threshold by one step of the grayscale ( $\frac{1}{256}$ ) resulted in a change of the value of SiC particle volume by  $\pm 0.9\%V$ . Lower resolution of tomography, compared to optical microscopy, resulted in the lack of the smallest particle group in the tomographic spectrum, with the volume around  $0.2\%V$ . Consequently, the total error of the method was determined at the level of  $\Delta V = \pm 1.1\%$ .

The remaining error may be connected to the preparation procedures of Cu/SiC composites. The character of errors related to the determination of SiC particle coordinates was the result of the algorithm separating the connected particles. It was determined that the best particle separation algorithm would be the one for which volumetric spectra of particles would be similar. It was assumed that the lowest separation error concerned the composite with the lowest phase share 10vol.% SiC. Out of the various tested algorithms, similar volume distributions of SiC particles (Fig. 7) for all four samples were obtained basing on the Integrating Concave Points Clustering and Random Walker Algorithm (He Y. *et al.*, 2014). In absolute values, the error in values of particle coordinates was not determined. Error analysis of the measurement of the volume share of the SiC phase, as well as selecting the algorithm of particle separation was conducted for the composite layers with the following dimensions –  $2000 \times 2000 \times 200 \mu\text{m}^3$ .

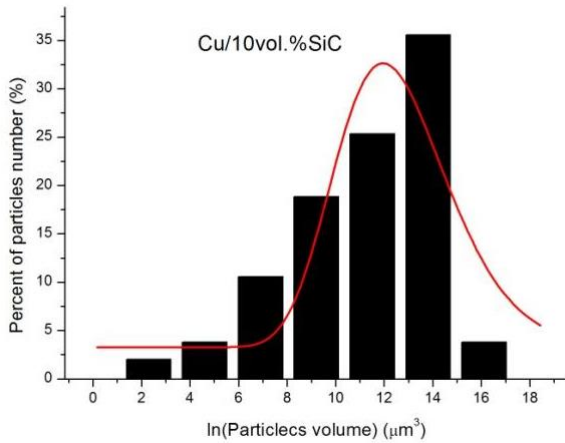


Fig. 7. *Distribution of the volume of SiC particles.*

Fig. 8 presents the distribution of coordinates of the centers of mass of SiC particles in the layers of the studied samples. The largest diffusion of coordinates is found in the composite with the lowest, 10vol.% volume fraction of the SiC phase. For the isotropic material, the coordinates of the centers of mass should have the values of  $x_c = y_c = z_c = 0$ .

The Cu/30vol.%SiC composite was identified as the most isotropic material – Table 1. It can be also found that the isotropy of the material increases with the increase of the volume fraction of the reinforcing phase. In the Cu/40vol.%SiC material, the differences in the coordinates of the centers of mass, compared to the Cu/30vol.%SiC composite, are small but further research reveals significant changes of SiC particles along Z-axis dependence. They may result from a small, linear gradient of a particle mass distribution, presented in Fig. 6, as the inclination of a straight line that approximates the experimental data.

Theoretically, moments of inertia of masses, measured in an external coordinate system (Fig. 9) related to the uniform samples, should be identical – therefore, their quotients should be identical. In order to compare homogeneity parameters of the analyzed samples the average value and standard deviation of moment quotient was calculated and compared in Table 1.

Table 1. *Average density of SiC, coordinates of mass center and momentum of inertia determined from 3D reconstruction of Cu/SiC composite materials.*

Result	10vol.%SiC	20vol.%SiC	30vol.%SiC	40vol.%SiC
Volume fraction of SiC, $V_V(\%)$	9.07	18.64	28.31	36.62
Relative coordinates of mass centers $\begin{pmatrix} x_c \mu\text{m} \pm \text{std. err. } \mu\text{m} \\ y_c \mu\text{m} \pm \text{std. err. } \mu\text{m} \\ z_c \mu\text{m} \pm \text{slope} \frac{\%}{\mu\text{m}} \times 10^{-4} \end{pmatrix}$	$\begin{pmatrix} 69.7 \pm 63.7 \\ 15.9 \pm 64.2 \\ -18.64 \pm 5.84 \end{pmatrix}$	$\begin{pmatrix} 77.3 \pm 41.5 \\ -11.6 \pm 37.5 \\ -321.14 \pm 24.6 \end{pmatrix}$	$\begin{pmatrix} -55.4 \pm 25.7 \\ -60.1 \pm 29.7 \\ -8.84 \pm 2.76 \end{pmatrix}$	$\begin{pmatrix} 4.3 \pm 29.6 \\ 42.3 \pm 40.3 \\ -292.24 \pm 74.5 \end{pmatrix}$
Avg. inertia moment quotient $M_{x/y} \pm \text{std. err.}$	$1.38 \pm 0.23$	$1.15 \pm 0.10$	$1.10 \pm 0.03$	$1.09 \pm 0.04$

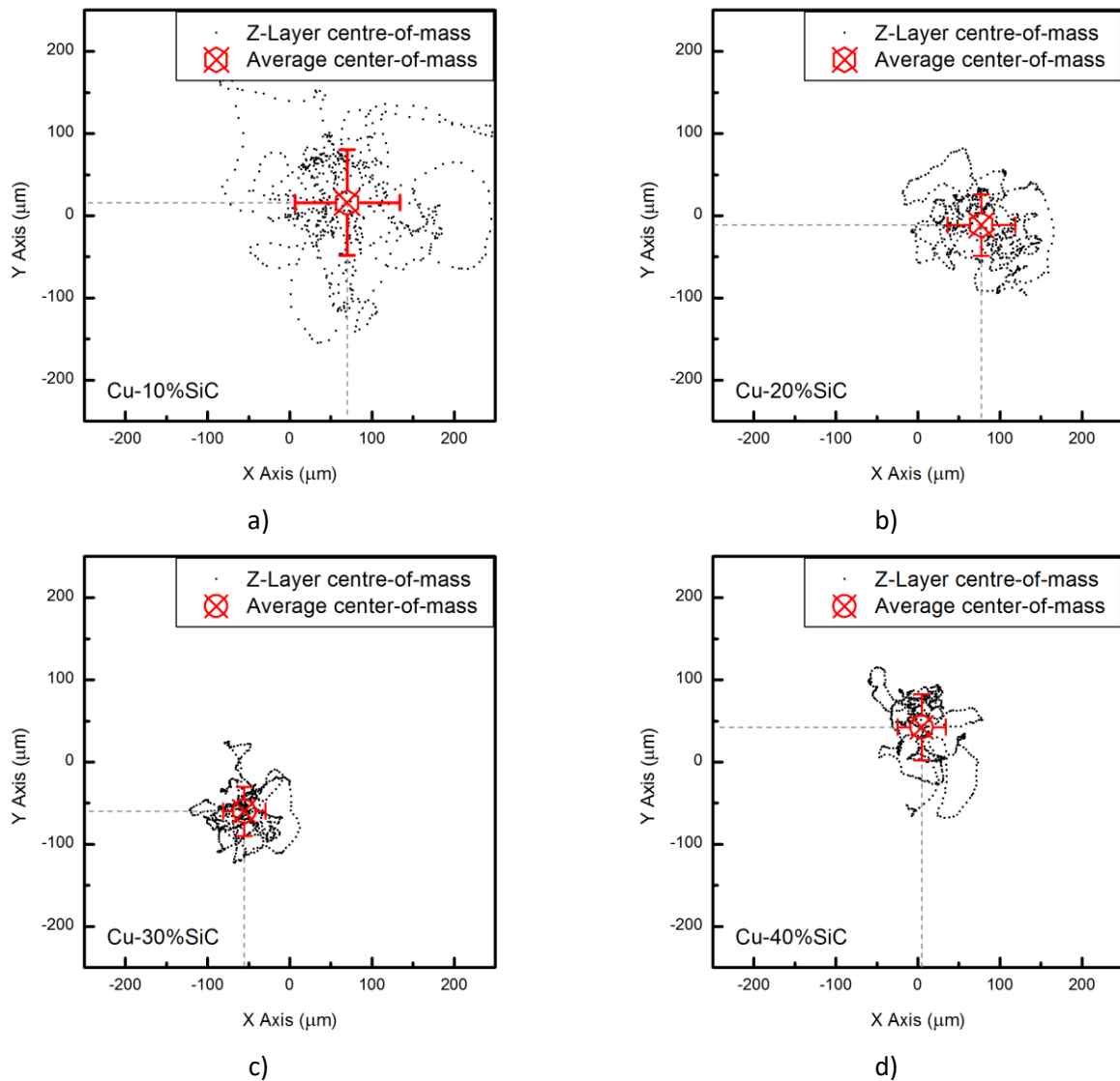


Fig. 8. Distribution of mass centers coordinates in layers cutting in the direction of the Z axis. Samples a) Cu/10vol.%SiC; b) Cu/20vol.%SiC; c) Cu/30vol.%SiC; d) Cu/40vol.%SiC.

Summing up the numerical results of research include in Table 1, it must be pointed out that the values of the volume fraction of the SiC phase  $V_{SiC}(\%)$ , within the margin of error  $\Delta V = \pm 1.1\%V$ , are consistent with the conditions of the experiment. The differences in the determined coordinates of the

centers of mass  $(x_c; y_c; z_c)$  for the Cu/10vol.%SiC and Cu/20vol.%SiC samples are significantly larger than in other two cases. Therefore, it should be assumed that within four studied samples, only Cu/30vol.%SiC is isotropic and uniform.

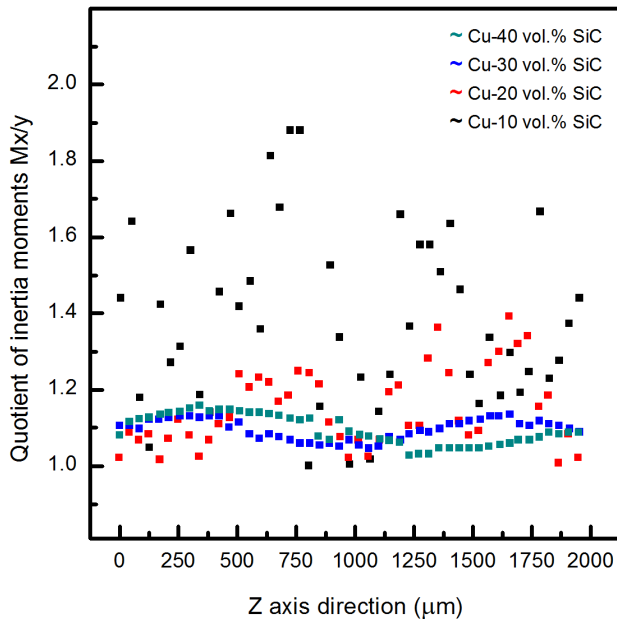


Fig. 9. *Distribution of inertia moments quotients in layers cutting in the direction of the Z axis.*

## SUMMARY AND CONCLUSIONS

Microtomography methods are undoubtedly a powerful tool in material research. At the same time, their use in quantitative structural analysis is a technically complicated process, mainly due to the separation of 3D-connected particles of shapes other than spherical, in various orientations. Ultimately, quantitative analysis of studied Cu/SiC structures was conducted in the looped procedure system: separation of flat images, 3D reconstruction, calculation of particle volume, analysis of distributions of SiC particle volumes and their number. The results obtained by extensive analysis shown a general trend where increasing volume fraction of SiC resulted in higher isotropy and homogeneity of SiC/Cu composites. The results are logically consistent with the thesis that two materials with similar particle shapes and sizes may be well mixed in a gravitational field, even with differing specific weights. In addition, an increase in the density of the reinforcing phase, provided the components are uniformly mixed, must increase its isotropy, within the identical – with respect to size and shape – spaces of composite formation. The mechanical and thermal loading applied during materials fabrication had a lesser impact on the translational or rotational motion of powder particles

as their volume fraction in the material raised. Gravitational segregation along Z axis is also visible and was not significant only in the 30vol.%SiC composition.

## ACKNOWLEDGEMENT

The studies have been carried out as a part of the project entitled “The correlation between interface morphology and heat transfer in Cu-SiC composites in function of the form of reinforcement material” financed by the National Science Center within the framework of OPUS Programme (contract ref. no.: 2014/13/B/ST8/04320)

## REFERENCES

- Barmouz M., Araee A. (2014) Effect of SiC particles dispersion on the grain size and mechanical properties of Cu/SiC metal matrix nanocomposites produced via MFSP", *J Nano Res* 26:53-8.
- Besharati M.K., Taherishargh G.M. (2011) Investigation of mechanical properties of Cu/SiC composite fabricated by FSP: effect of SiC particles' size and volume fraction. *Mater Sci Eng: A* 528(3):1740-9.
- Campbell F.C. (2010) *Introduction to Composite Materials Structural Composite Materials*. ASM International® <http://www.asminternational.org>
- Chmielewski M., Pietrzak K., Strojny-Nędza A., Jarzabek D., Nosewicz S., (2017) Investigations of interface properties in copper-silicon carbide composites. *Arch Metall Mater* 62(2B):1315-8.
- Chmielewski M., Pietrzak K., Teodorczyk M., Nosewicz S., Jarzabek D., Zybała R., Bazarnik P., Lewandowska M., Strojny-Nędza A. (2017) Effect of metallic coating on the properties of copper-silicon carbide composites. *Appl Surf Sci* 421A:159-69.
- DeHoff R.T., Rhines F.N. (1961) Determination of the number of particles per unit volume from measurements made on random plane section: the general cylinder and the ellipsoid. *Trans AIME* 221:975-82.
- Gan K., Gu M. (2008) The compressibility of Cu/SiC powder prepared by high-energy ball milling. *J Mater Process Tech* 199 (1-3):173-7.
- Gawdzińska K., Wojnar L., Maliński M., Chrapoński J. (2010) Structure homogeneity as a parameter for evaluation of composite casting quality. *Archives of Foundry Engineering* 10(3):187-92.



- Głowacz E., Czarski A. (2008) Scheil-Schwartz-Saltykov method in the matrix depiction. *Inżynieria Materiałowa* 29(4):418-20.
- He Y., Meng Y., Gong H., Chen S., Zhang B., Ding W., Luo Q., Li A. (2014) An automated three-dimensional detection and segmentation method for touching cells by integrating concave points clustering and random walker algorithm., *PLOS One* 9(8).
- Iguchi M., Suehirto T., Watanabe Y. (1982) Composite materials reinforced with polyoxymethylene whiskers. *J Mater Sci* 17:1632-8.
- Jarzabek D., Chmielewski M., Dulnik J., Strojny-Nedza A. (2016) The influence of the particle size on the adhesion between ceramic particles and metal matrix in MMC composites. *J Mater Eng Perform* 25(8):3139-45.
- Kimoto T., Cooper J. A. (2014) *Fundamentals of Silicon Carbide Technology: Growth, Characterization, Devices, and Applications*, Major Physical Properties of Common SiC Polytypes, First Edition Published by John Wiley & Sons Singapore Pte Ltd. 7.
- Maire E., Withers P. J. (2014) Quantitative X-ray tomography. *Int Mater Rev.* 59(1):1-43, 23.
- Pietrzak K., Sobczak N., Chmielewski M., Homa M., Gazda A., Zybala R., Strojny-Nędza A. (2016) Effects of carbon allotropic forms on microstructure and thermal properties of Cu-C composites produced by SPS. *J Mater Eng Perform* 25(8):3077-83.
- Schubert Th., Brendel A., Schmid K., Koeck Th., Ciupiński Ł., Zieliński W., Weißgärber T., Kieback B. (2007) Interfacial design of Cu/SiC composites prepared by powder metallurgy for heat sink applications. *Compos Part A-Appl S.* 38(12):2398-403.
- Singh H., Kumar L., Alam S. N. (2015) Development of Cu Reinforced SiC Particulate Composites. 4<sup>th</sup> National Conference on Processing and Characterization of Materials IOP Conf. Series: Mater Sci Eng. 75.
- Srinivasan C., Karunanithi M. (2015) Fabrication of surface level Cu/SiCp nanocomposites by friction stir processing route. *J Nanotechnol.* Article ID 612617:1-10 13.
- Underwood E.E. (1970) *Quantitative Stereology*, Addison-Wesley; Massachusetts, U.S.A.
- Weber L., Tavangar R. (2007) On the influence of active element content on the thermal conductivity and thermal expansion of Cu-X (X = Cr, B) diamond composites. *Scripta Mater* 57:988-91.
- Wejrzanowski T., Spsychalski W.L., Roźniatowski K., Kurzydłowski K.J., (2008), Image based analysis of complex microstructures of engineering materials. *Int J Appl Math Comp.* 18(1):33-9.
- Wejrzanowski T., Lewandowska M., Kurzydłowski K.J., (2010), Stereology of nanomaterials., *Image Anal Stereol* 29:1-12.
- Xu Y.H., Pitot H.C. (2003) An improved stereologic method for three-dimensional estimation of particle size distribution from observations in two dimensions and its application. *Comput Meth Prog Bio* 72(1):1-20.
- Yoshida K., Morigami H. (2004) Thermal properties of diamond/copper composite material. *Microelectron Reliab* 44:303-8.
- Zaman M., Bukhari S.N.S., Ir M., Brabazon D., Hashmi M.S.J. (2012) Evaluation on metal matrix composite of CuSiC as candidate for thermal management materials in electronics packaging. The 2nd International Malaysia-Ireland Joint Symposium on Engineering, Science and Business 2012.
- Zhan Y., Zhang G. (2003) The effect of interfacial modifying on the mechanical and wear properties of SiC p/Cu composites. *Mater Lett.* 57:4583.